

UNCLASSIFIED

Defense Technical Information Center
Compilation Part Notice

ADP012373

TITLE: CFD Simulation of Liquid Rocket Engine Injectors. Part 3.
Simulations of the RCM-3 Experiment

DISTRIBUTION: Approved for public release, distribution unlimited

This paper is part of the following report:

TITLE: 2nd International Workshop on Rocket Combustion Modeling:
Atomization, Combustion and Heat Transfer held in Lampoldshausen,
Germany on 25-27 Mar 2001

To order the complete compilation report, use: ADA402618

The component part is provided here to allow users access to individually authored sections of proceedings, annals, symposia, etc. However, the component should be considered within the context of the overall compilation report and not as a stand-alone technical report.

The following component part numbers comprise the compilation report:
ADP012355 thru ADP012373

UNCLASSIFIED

CFD SIMULATION OF LIQUID ROCKET ENGINE INJECTORS

Part 3. SIMULATIONS OF THE RCM-3 EXPERIMENT

Richard Farmer & Gary Cheng
SECA, Inc.

Yen-Sen Chen
ESI, Inc.

INTRODUCTION

Detailed design issues associated with liquid rocket engine injectors and combustion chamber operation require CFD methodology which simulates highly three-dimensional, turbulent, vaporizing, and combusting flows. The primary utility of such simulations involves predicting multi-dimensional effects caused by specific injector configurations. SECA, Inc. and Engineering Sciences, Inc. have been developing appropriate computational methodology for NASA/MSFC for the past decade. CFD tools and computers have improved dramatically during this time period; however, the physical submodels used in these analyses must still remain relatively simple in order to produce useful results. Simulations of clustered coaxial and impinger injector elements for hydrogen and hydrocarbon fuels, which account for real fluid properties, is the immediate goal of this research. The spray combustion codes are based on the FDNS CFD code¹ and are structured to represent homogeneous and heterogeneous spray combustion. The homogeneous spray model treats the flow as a continuum of multi-phase, multicomponent fluids which move without thermal or velocity lags between the phases. Two heterogeneous models were developed: (1) a volume-of-fluid (VOF) model which represents the liquid core of coaxial or impinger jets and their atomization and vaporization, and (2) a Blob model which represents the injected streams as a cloud of droplets the size of the injector orifice which subsequently exhibit particle interaction, vaporization, and combustion. All of these spray models are computationally intensive, but this is unavoidable to accurately account for the complex physics and combustion which is to be predicted. Work is currently in progress to parallelize these codes to improve their computational efficiency.

These spray combustion codes were used to simulate the three test cases which are the subject of the 2nd International Workshop on Rocket Combustion Modeling. Such test cases are considered by these investigators to be very valuable for code validation because combustion kinetics, turbulence models and atomization models based on low pressure experiments of hydrogen air combustion do not adequately verify analytical or CFD submodels which are necessary to simulate rocket engine combustion.

We wish to emphasize that the simulations which we prepared for this meeting are meant to test the accuracy of the approximations used in our general purpose spray combustion models, rather than represent a definitive analysis of each of the experiments which were conducted. Our goal is to accurately predict local temperatures and mixture ratios in rocket engines; hence predicting individual experiments is used only for code validation. To replace the conventional JANNAF standard axisymmetric finite-rate (TDK) computer code² for performance prediction with CFD cases, such codes must possess two features. Firstly, they must be as easy to use and of comparable run times for

conventional performance predictions. Secondly, they must provide more detailed predictions of the flowfields near the injector face. Specifically, they must accurately predict the convective mixing of injected liquid propellants in terms of the injector element configurations.

HOMOGENEOUS SPRAY COMBUSTION MODEL

The homogeneous spray combustion CFD codes utilize very general thermodynamics in a conventional CFD code. The heterogeneous codes (described in Part 2) use tabulated properties for the liquid phase and ideal gas properties for the vapor phase. Thermal and caloric equations of state, vapor pressure, heat of vaporization, surface tension, and transport properties are modeled with the equations of state proposed by Hirshfelder, et al^{3,4} (we term these the HBMS equations of state) and with conventional correlations,⁵ for the other properties. The property correlations used were not chosen for their absolute accuracy, but for their validity over a wide range of temperatures and pressures and for requiring a minimum of data to describe a particular species. These correlations are explicit in density and temperature.

HBMS thermal equation of state:

$$\frac{P}{P_c} = \sum_{j=1}^4 T_r^{j-2} \sum_{i=1}^6 B_{ij} \rho_r^{i-2} ; T_r = \frac{T}{T_c} ; \rho_r = \frac{\rho}{\rho_c}$$

HBMS caloric equation of state:

$$\frac{H - H_0}{RT} = Z_c \int_0^{\rho_r} \left[\frac{P}{T_r} - \left(\frac{\partial P}{\partial T_r} \right)_{\rho_r} \right] \rho_r^{-2} d\rho_r + Z_c \frac{P}{\rho_r T_r} - 1$$

These equations are based on the "theorem of corresponding states" for real fluids, which essentially means that the p-v-T relations for all species are similar if these variables are normalized with their values at the critical point, i.e. if reduced values are used. The reduced values in these equations are indicated with a subscript r. H_0 is the ideal gas species enthalpy. Z_c is the compressibility for a given species at the critical point. The HBMS equations are attractive to use because arbitrary correlations for vapor pressure, heat of vaporization, and liquid densities can be used. Since multi-component fluid/vapor mixtures may be present in the flowfield, the mixture properties are calculated by the additive volume method. This means that multiphase mixtures are treated as ideal solutions. For H_2/O_2 propellants under conditions where the species become ideal gases, the thermodynamic data from the CEC code⁶ were used.

The combustion reactions used in the simulations reported herein are shown in Table 1. Not all of the reactions were used in all of the combustion simulations. Elementary rate data for these reactions are reported by Gardner, et al^{7,8}. Such data are empirical and were obtained for hydrogen/air combustion, under conditions far different from those encountered in rocket engines.

Table 1. Combustion Model for H₂/O₂ Reaction

Chain initiation: $\text{H}_2 + \text{O}_2 = 2\text{OH}$ $1.86 \text{ H}_2 + \text{O}_2 = 1.645 \text{ H}_2\text{O} + 0.067 \text{ O} + 0.142 \text{ H} + 0.288 \text{ OH}$
Chain Branching: $\text{H}_2 + \text{OH} = \text{H}_2\text{O} + \text{H}$ $2 \text{ OH} = \text{H}_2\text{O} + \text{O}$ $\text{H}_2 + \text{O} = \text{H} + \text{OH}$ $\text{O}_2 + \text{H} = \text{O} + \text{OH}$
Chain termination: $\text{O} + \text{H} + \text{M} = \text{OH} + \text{M}$ $2 \text{ O} + \text{M} = \text{O}_2 + \text{M}$ $2 \text{ H} + \text{M} = \text{H}_2 + \text{M}$ $\text{OH} + \text{H} + \text{M} = \text{H}_2\text{O} + \text{M}$

The CFD solver used was the Finite-Difference Navier-Stokes code with provision for using real fluid properties, the FDNS-RFV code. This code is pressure based; it differs from an ideal gas code in the methodology used to relate the pressure correction to the continuity equation and of course in the properties subroutines used. The pressure correction (p') equation used in the FDNS-RFV code is:

$$\frac{\beta_p p'}{\Delta T} \Delta \bullet (u_i \beta_p p') - \Delta \bullet (\rho^* D_p \Delta p') = - \Delta \bullet (\rho^* u_i) - \frac{\rho^* - \rho^n}{\Delta t}$$

$$p^{n+1} = p^n + p' ; \quad \beta_p = \gamma / a^2 ; \quad u_i \approx - D_p \Delta p'$$

where the superscripts * and n denote the value at the intermediate and previous time steps, respectively. D_p is the inverse of the matrix of the coefficients of the convective terms in the finite-difference form of the inviscid equations of motion. This is not an obvious definition, but is one which has made the FDNS-RFV code a useful solver. The sound speed used in the pressure correction equation is that calculated for the real fluid multi-component mixture.

In all cases simulated, a k-ε turbulence model was used to close the mass averaged transport equations solved by the code. Our experience is that this incompressible turbulence model overestimates the mixing in a combustng flowfield. However, since the liquid propellants are also mixed by this model, we concluded that there are currently insufficient data to better tune the turbulence model. The homogeneous spray model has been used to simulate: (1) a single element like-on-like (LOL) impinger injector element and a single element unlike impinger element for the configuration and flow conditions used in the cold-flow experiments; (2) an ensemble of injector elements in the Fastrac engine; and (3) several configurations of the vortex engine currently being developed.⁹

RESULTS

The super-critical combustion case, RCM-3, was simulated with the homogeneous spray combustion model. Any drops present will be highly unstable; therefore, this model should represent the flow rather well. Local equilibrium and simplified finite-rate combustion submodels were used and the results for the two simulations compared well. More detailed combustion submodels were attempted, but proved to behave too poorly for successful simulations.

The preponderance of super-critical spray combustion models which have been reported have been extensions of sub-critical models. Such models encounter a basic problem in over emphasizing the role of surface tension. Since surface tension is zero for super-critical conditions, drops should not exist. Although such drops can be observed experimentally, they are extremely unstable and do not survive very long. The homogeneous CFD model was developed to account for the major physical effects which do exist. Namely, the large density and momentum differences which exist in multi-phase super-critical flows. Such a model allows one to accurately relate the inlet conditions at the injector face to boundary conditions for the CFD simulation. This relationship is essential to predicting the effects of injector element configuration and inlet momentum vector on the convective mixing and cross winds which occur in practical rocket engines. Otherwise, one is forced to use the historical method of creating costly experimental data bases from which to choose designs.

The injector configuration and flow conditions for the supercritical combustion of the RCM-3 test case are presented in Fig. 1. This is uni-element shear coaxial injector with LOX and GH_2 propellants. The numerical simulation was conducted with some simplification because, initially, detailed information was unavailable; such as: (1) the flare of LOX injector near the exit was neglected; (2) the injector was flush at the chamber head-end instead of protruding into the chamber because the outer diameter of hydrogen tube and distance between the chamber head-end and the injector exit were not known; (3) the nozzle was not included because of insufficient information about the chamber tail-end and nozzle geometry; and (4) the coolant (later found to be helium) for the chamber wall was not included because its flow rate and properties were not specified. As can be seen, the chamber pressure (60 bar) is well above the critical pressure of oxygen; hence, the homogeneous real-fluid model was used to simulate this test case. A two-zone mesh system (61x39 and 301x101) was used to model the injector section and the combustion chamber.

The combustion reactions in this high pressure experiment are expected to be in local thermodynamic equilibrium and were simulated as such. To demonstrate the methodology, two finite-rate simulations were also made with a subset of the reactions in Table 1. The single global reaction which produces radicals as well as water provides a good estimate of the temperature field. Its rate was set to attach the flame near the injector tip. Since the radicals are not rigorously simulated with the single reaction, a second finite-rate simulation was made with the 2-body reactions. Backward reaction rates are determined with equilibrium constants. A third finite-rate/equilibrium model was also tested. The finite-rate effects were described with the 9 elementary reactions in Table 1 with the combustion assumed to be in local equilibrium when the temperature was greater than some specified value. Temperatures of 1000 and 1500K were used for this switch point. Thus, the finite-rate effects would be considered near the injector and in the expansion section of the nozzle. This combustion model did not require an extremely tight grid near the injector tip to hold the flame. The simulation of the RCM-3 case with this model was very similar to the equilibrium combustion

model For high pressure cases such combustion modeling is essential to keep the computation stable.

The chemistry and turbulence models used in our simulations do not make use of probability density functions (PDFs) because most of the shear layers formed by the injector element should be continuum. The only regions for which this might not be the case are the intermittent edges of the shear layers. Pope¹⁰ terms these regions the "viscous superlayer". The thickness of these layers are inversely proportional to the Reynolds number to the 0.75 power. For these high speed coaxial jets, they should be very thin.

The flow predicted at the injector tip is shown in Figure 2. The radial temperature profiles predicted at several axial stations are shown in Figure 3. The axial profiles at several radial locations are shown in Figure 4. The temperature and oxygen and OH concentration profile fields are shown in Figure 5. The combustion models used do not predict chemiluminescent OH, which might be observed in the experiments. These results are shown for the equilibrium combustion model. Results for the finite-rate equilibrium combustion simulations are very similar, hence they are not shown.

The wall temperature distributions for all four cases are compared in Figure 6, and as noted the results are very similar.

CONCLUSIONS

The following conclusions were drawn from performing CFD simulations of the three RCM test cases for the 2nd IWRCM.

1. A homogeneous and a heterogeneous spray combustion CFD models have been developed to simulate combustion in rocket engines. Since neither of these models is expected to be accurate until critical parameters are evaluated from test data, simulation comparisons to the MASCOTTE type experiments are needed.
2. The utility of either CFD model cannot be determined until values of critical parameters are determined and efforts to optimize the computational efficiency of the models are performed.
3. Although the CFD rocket engine models provide much more detailed information concerning the vaporization, mixing, and combustion process, their place in the design process is yet to be identified. Older more approximate rocket "performance" models are difficult to displace. Furthermore, every physical process thought to be present in the engine does not have to be modeled to create a useful design code. There are more knobs to adjust in the code than there are experimental data to justify their turning.
4. The experiments conducted in preparation for the 2nd IWRCM appear to be a significant first step in providing test data valuable to CFD modelers. However, blind comparisons of CFD model predictions to such data are premature. The CFD modelers have not previously had sufficient test data properly specify the many assumptions which are necessary to simulate such complex flows.
5. Better communication between analysts and experimenters needs to be accomplished. Can the modeler simulate the experiments which are being performed? Can the data obtained from the experiment critically test the model?

ACKNOWLEDGEMENTS

The authors wish to express their appreciation to Mr. Robert Garcia and Dr. Bill Anderson for their encouragement and support. This work was performed under NAS8-00162 for the Marshall Space Flight Center of the National Aeronautics and Space Administration.

REFERENCES

1. Chen, Y.S., "Compressible and Incompressible Flow Computations with a Pressure Based Method," AIAA Paper 89-0286, 1989.
2. Nickerson, G.R., et al, "Two-Dimensional Kinetics (TDK) Nozzle Performance Computer Program," Vols. I-III, Rpt. No. SN91, Software and Engineering Associates, Inc., mar. 1989.
3. Hirschfelder, J.O., et al, "Generalized Equations of State for Gases and Liquids," IEC, 50, pp.375-385, 1958.
4. Hirschfelder, J.O., et al, "Generalized Excess Functions for Gases and Liquids," IEC, 50, pp.386-390, 1958.
5. Reid, R.C., et al, The Properties of Gases & Liquids, 4th ed, McGraw-Hill, 1987.
6. Gordon, S., and B.J. McBride, "Computer Program for Calculation of Complex Chemical Equilibrium Compositions, Rocket Performance, Incident and Reflected Shocks, and Chapman-Jouget Detonations," NASA-SP-273, 1971.
7. Gardiner, W.C., Jr., Combustion Chemistry, Springer-Verlag, 1984.
8. Gardiner, W.C., Jr., Ed., Gas-Phase Combustion Chemistry, Springer, 1999.
9. Farmer, R.C, G. Cheng, H. Trinh, and K. Tucker, "A Design Tool for Liquid Rocket Engine Injectors," AIAA 2000-3499, 2000.
10. Pope, S.B., Turbulent Flows, Cambridge, 2000.

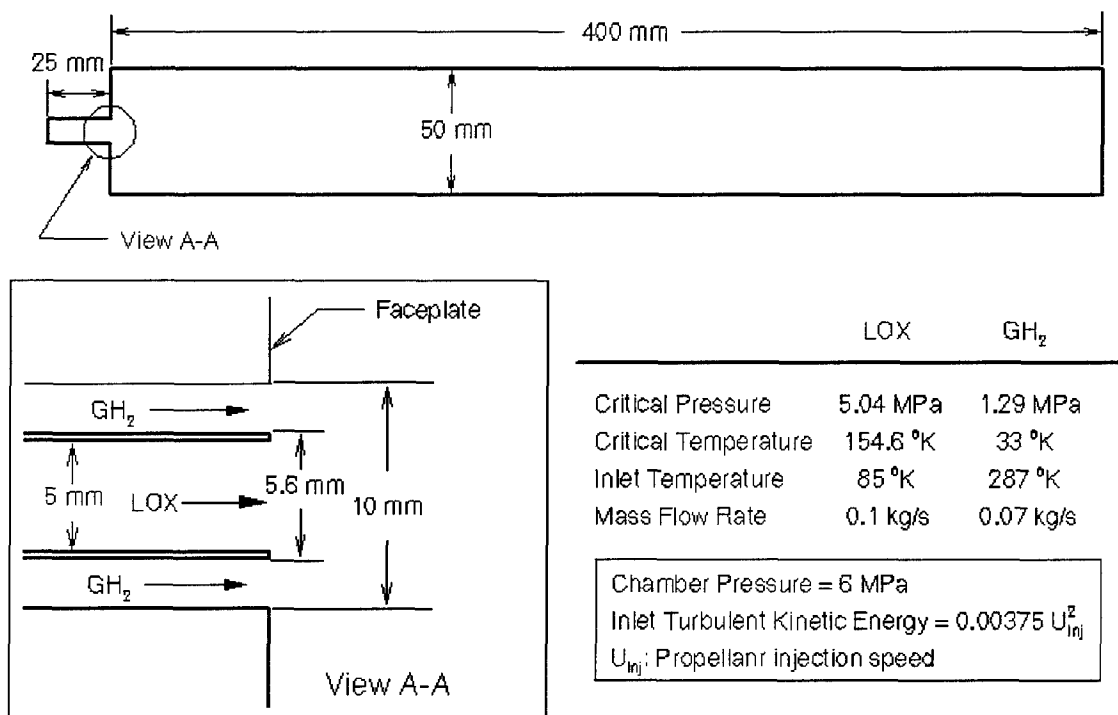


Figure 1. Configuration of the RCM-3 Case (Homogeneous Spray Model).

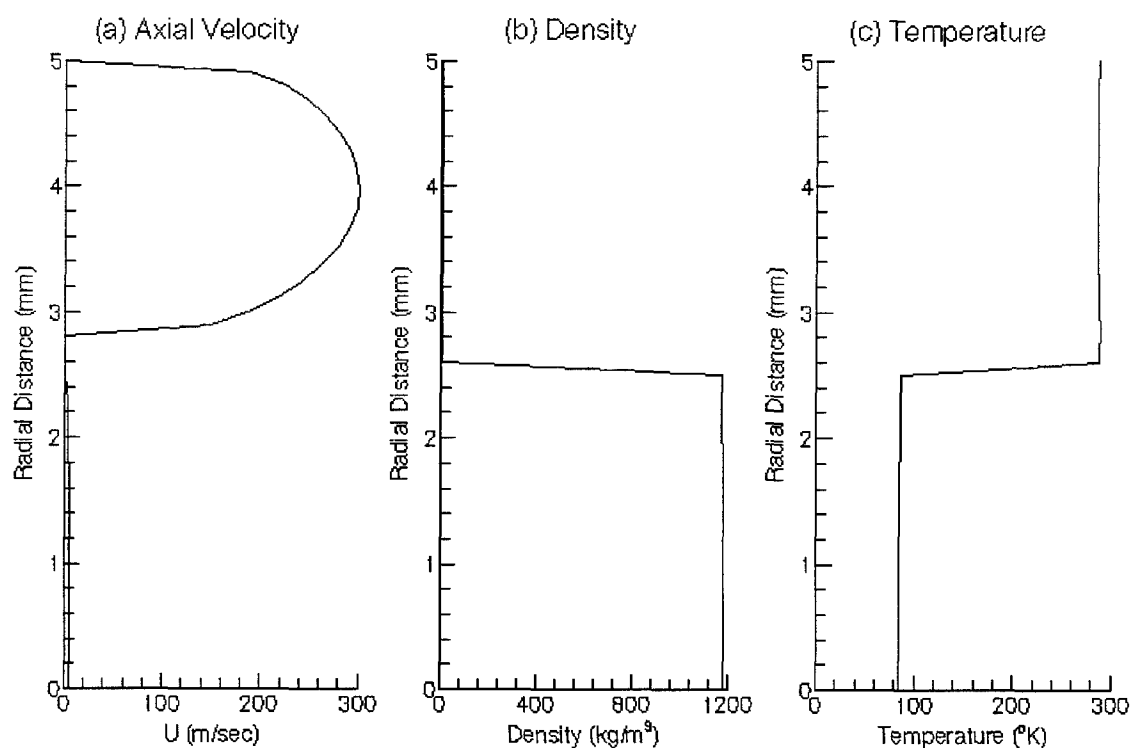


Figure 2. Flow Properties at the Injector Exit of RCM-3 (Homogeneous Spray Model).

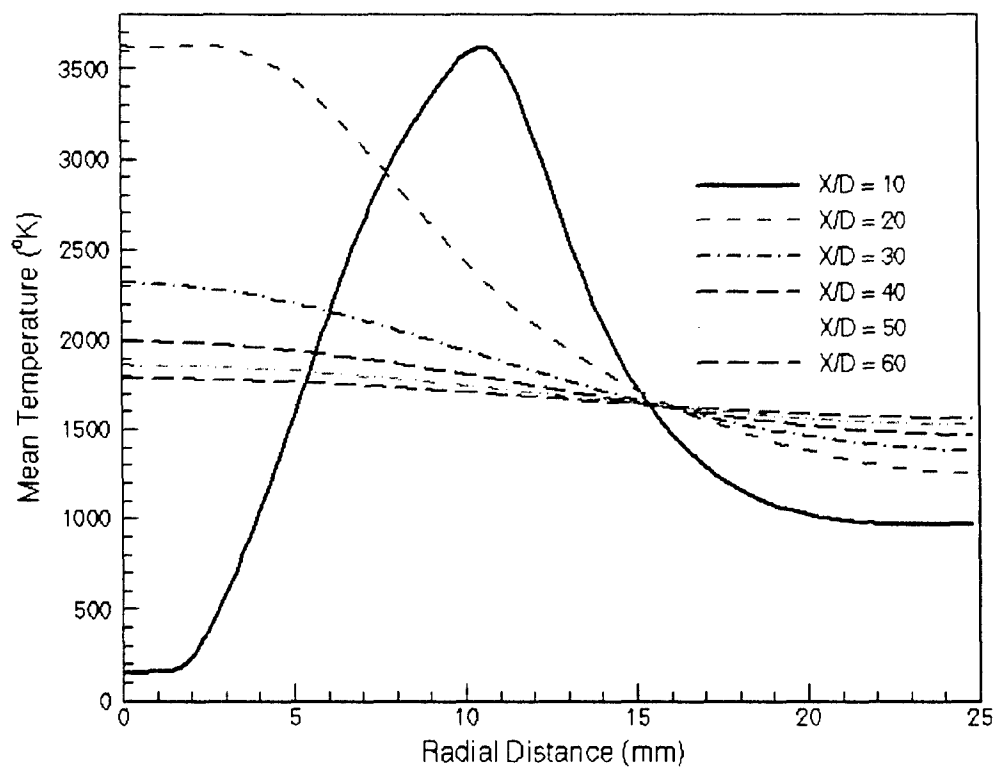


Figure 3. Radial Profiles of Mean Temperature at Various Axial Locations of RCM-3.

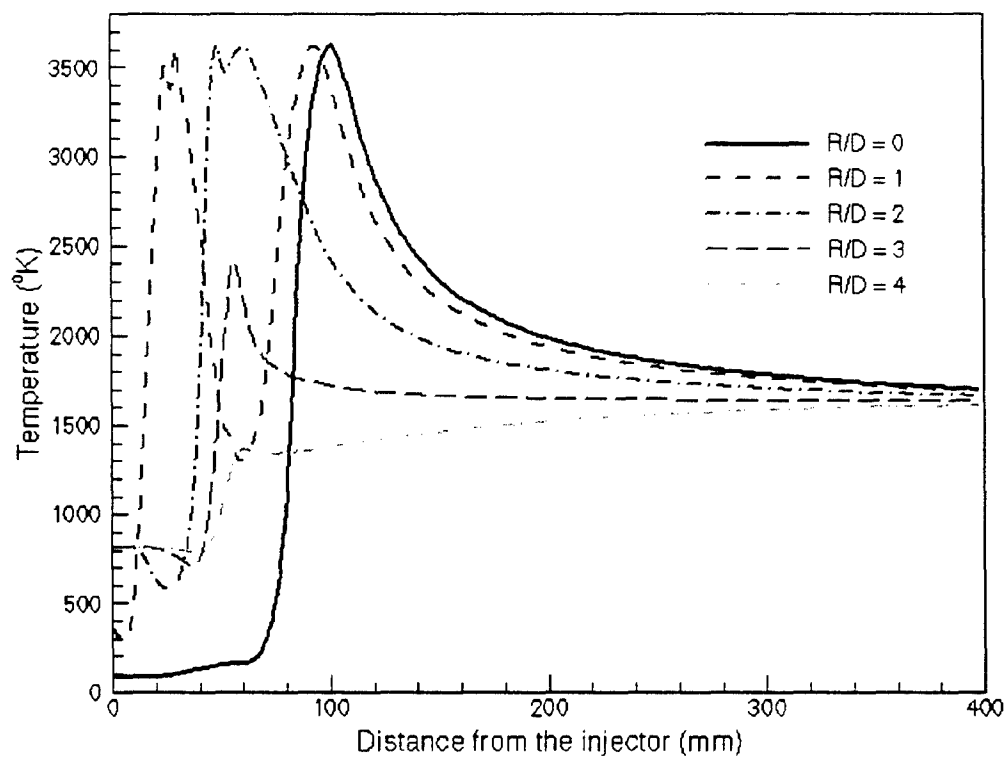


Figure 4. Axial Profiles of Mean Temperature at Various Radial Locations of RCM-3.

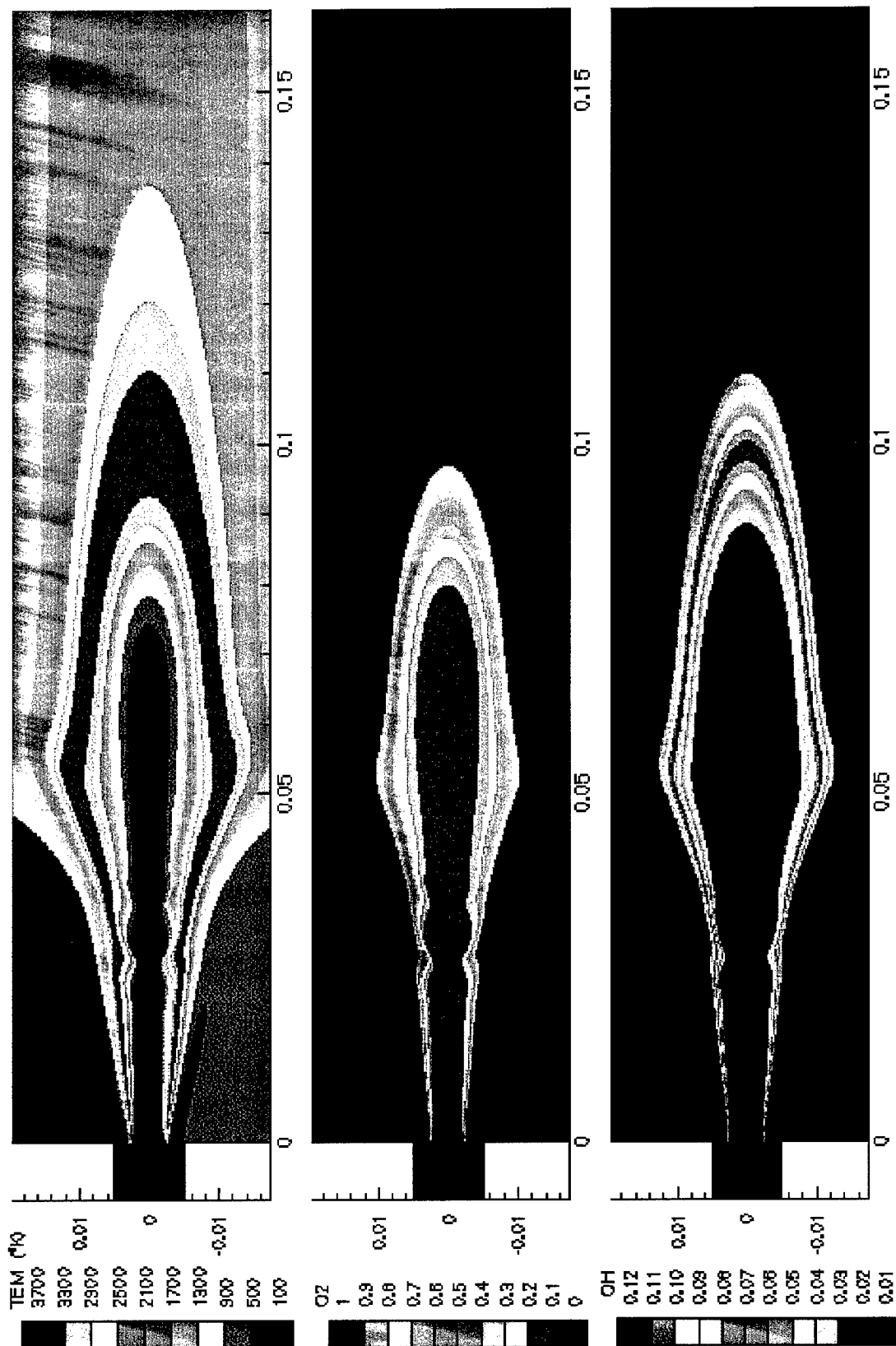


Figure 5. Temperature and Species Concentrations Near the Injector of RCM-3.

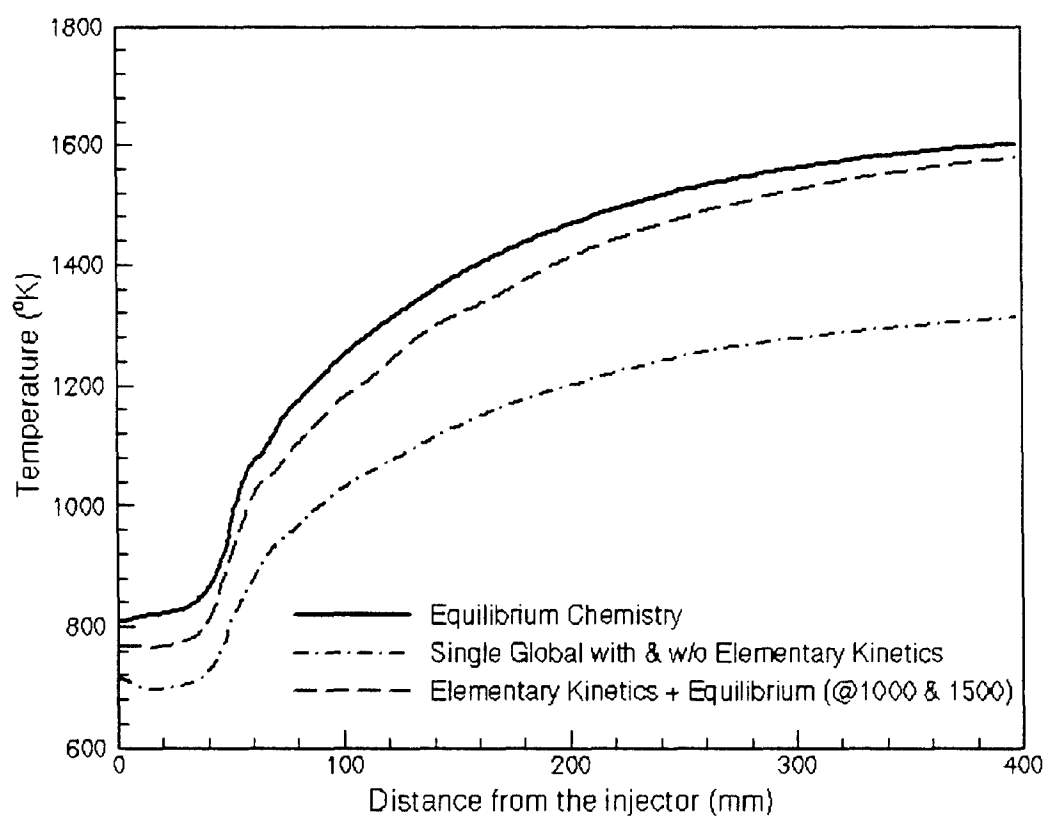


Figure 6. Near Wall Temperature Distributions for Various Chemistry Model of RCM-3.